POPULATION ECOLOGY - ORIGINAL PAPER

Demography of Verreaux's sifaka in a stochastic rainfall environment

Richard R. Lawler · Hal Caswell · Alison F. Richard ·
Joelisoa Ratsirarson · Robert E. Dewar ·
Marion Schwartz

Abstract In this study, we use deterministic and stochastic models to analyze the demography of Verreaux's sifaka (*Propithecus verreauxi verreauxi*) in a fluctuating rainfall environment. The model is based on 16 years of data from Beza Mahafaly Special Reserve, southwest Madagascar. The parameters in the stage-classified life cycle were estimated using mark-recapture methods. Statistical models were evaluated using information-theoretic techniques and multi-model inference. The highest ranking model is time-invariant, but the averaged model includes rainfall-dependence of survival and breeding. We used a time-series model of rainfall to construct a stochastic demographic model. The time-invariant model and the stochastic model give a population growth rate of about 0.98. Bootstrap confidence intervals on the growth rates, both deterministic and stochastic, include 1. Growth rates are most elastic to changes in adult survival. Many demographic statistics show a nonlinear response to annual rainfall but are depressed when annual rainfall is low, or the variance in annual rainfall is high. Perturbation analyses from both the time-invariant and stochastic models indicate that recruitment and survival of older females are key determinants of population growth rate.

Keywords Lemurs · Madagascar · Mark-recapture · Climate · Time-series

Communicated by Jörg Ganzhorn.

R. R. Lawler (✉)
Department of Anthropology,
Boston University, Boston, MA 02215, USA
e-mail: rlawler@bu.edu

R. R. Lawler · H. Caswell
Biology Department, Woods Hole Oceanographic Institution,
Woods Hole, USA

A. F. Richard
Vice Chancellor's Office, University of Cambridge,
Cambridge, UK

J. Ratsirarson
Departement des Eaux et Forets, E.S.S.A.,
Universite d'Antananarivo, Antananarivo, Madagascar

R. E. Dewar
Department of Archaeology, University of Cambridge,
Cambridge, UK

M. Schwartz
Department of Anthropology, Yale University,
New Haven, USA

Present Address:
R. R. Lawler
Department of Anthropology, James Madison University,
Harrisonburg, USA

Introduction

Almost one-third of the world's primate species are classified as threatened or worse (Cowlishaw and Dunbar 2000; Strier 2007); among the most endangered primates are some of the lemurs of Madagascar (Mittermeier et al. 2006). Demographic studies of wild primates can be used to understand the factors that shape primate population dynamics and contribute to conservation strategies. A demographic analysis must include information on age- or stage-specific survival, development, and fertility (i.e., the population's vital rates), throughout the life cycle. This information is the minimum permitting calculation of the rate of population growth and its response (via sensitivity or elasticity analysis) to perturbations. The perturbations

may include both natural environmental change and human management actions.

This kind of demographic information has been reported for only a few primate populations (excluding, of course, *Homo sapiens*). Alberts and Altmann (2003) presented a time-invariant model for the baboons in Amboseli and calculated the population growth rate and its sensitivity and elasticity to age-specific survival and fertility. Gage (1998) developed model life tables (age-specific survival and fertility) for four captive populations of New World monkey and several captive or provisioned (and one wild) populations of Old World monkey. He calculated the population growth rate and the periods of oscillations associated with subdominant roots. Dobson and Lyles (1989) performed a meta-analysis of primate life history data and estimated how the vital rates change with respect to sex ratio, social structure and density; they also included a qualitative assessment of how the vital rates are expected to respond to various environmental and anthropogenic perturbations. Other demographic studies of wild primates use a "bottom-up" approach, emphasizing connections between behavior, social structure, and the vital rates (e.g., Jolly et al. 2002; Gould et al. 2003; Pochron et al. 2004; Strier et al. 2006; Wich et al. 2007), but do not include sufficient information to calculate population growth rates and their response to perturbations.

Madagascar's lemurs constitute an endemic radiation of significant taxonomic and ecological diversity, and numerous studies have noted the unique life history schedules manifested by these primates when compared to mainland anthropoids (Richard and Dewar 1990; Kappeler 1996; Wright 1999). However, as Dewar and Richard (2007) note, Madagascar's mammalian taxa retain life history patterns qualitatively different from those of their mainland African counterparts and such life history schedules are not necessarily explained by isolation alone. Recently, several studies have either hypothesized or demonstrated a connection between rainfall and the unique life history schedules found among nonflying mammals in Madagascar (Wright 1999; Richard et al. 2002; Gould et al. 2003; Dewar and Richard 2007). In particular, rainfall in Madagascar is more unpredictable, both within and between years, than in other regions that experience similar median annual rainfall amounts (Dewar and Wallis 1999; Dewar and Richard 2007). Frequent cyclones and droughts occur throughout Madagascar and such stochastic occurrences influence the floristic heterogeneity and resource availability of Madagascar habitats (Ganzhorn 1995); in turn, the availability and quality of resources shape physiological, behavioral, and reproductive patterns in lemurs (Wright 1999; Richard et al. 2002; Gould et al. 2003; Dewar and Richard 2007). Because lemurs live in a highly variable environment, assessments of their population dynamics would benefit from an explicit analysis of demography with respect to environmental stochasticity.

In this paper, we present a stochastic demographic analysis of a wild lemur population. We develop a stage-classified model for the lemur Verreaux's sifaka (*Propithecus verreauxi verreauxi*), based on data from a wild, nonprovisioned population. We use multimodel inference (Burnham and Anderson 2002; Anderson 2008) to obtain estimates of demographic parameters and the response of those parameters to rainfall, accounting for the relative support by the data of a range of statistical models. We use this model to explore the effects of environmental variability on population dynamics. We focus on population growth rates (deterministic and stochastic, denoted as λ), their response to rainfall patterns, and the sensitivity of λ to changes in the sifaka life cycle. We focus on growth rates because they are critical to population viability, since changes in population size result from changes in growth rates. The models from which the growth rates are calculated are linear; if the population is at a density-dependent equilibrium, the growth rate is constrained to be 1. However, it is known that the sensitivity of the population growth rate at equilibrium is equivalent to the sensitivity of a weighted average (over stages) of population density (Caswell et al. 2004). So, analyses of population growth rate that focus on the effects of perturbations, either natural (e.g., rainfall) or human-induced (management) are still useful even if the true situation is one in which the population growth rate is constrained to 1.

Materials and methods

The species and life cycle

Verreaux's sifaka ("sifaka" hereafter) are diurnal, group-living, arboreal folivores inhabiting south and southwestern Madagascar. Sex ratios in social groups are generally equal and there is no sexual dimorphism between adult males and females. Sifaka have a brief 6–8 week mating season beginning mid January. Sifaka females may give birth as early as 3 years of age, but the average age at first birth is around 9 years of age. Infants are weaned after 6 months, and sifaka have been observed to survive up to 30 years in the wild. Their life history pattern comparatively falls on the "slow" end of the fast-slow continuum (Richard et al. 2000, 2002).

Our data come from a long-term study of a population of sifaka at Beza Mahafaly Special Reserve in southwest Madagascar. The sifaka population at Beza Mahafaly has been studied continuously since 1985. Individual animals are captured, marked, measured, and released back into the wild. Unmarked animals are captured each year using a

blow-pipe and tranquilizing dart; these individuals are usually unmarked yearlings and occasionally unmarked adult immigrants. For safety reasons, newborn infants are not captured and marked (they are captured a year later as yearlings). Each captured animal is measured and fitted with a color-coded collar and numbered tag. After recovery from the anesthetic the animal is released and rejoins its group. A full description of the capture protocol is given in Richard et al. (2002). Marked animals are subsequently censused and information about their status is noted. The population size fluctuates at around 280 animals, of which 80–90% are marked. There are approximately 50 social groups in the reserve at any time. From 1985 until 1992, the population was censused yearly, and from 1992 until the present, the population has been censused monthly. In this analysis, we use female release and resighting data from 1985 to 2001.

We classified individual females into stages based on age and reproductive status. In particular, we distinguish between mature females who reproduce in a given year and those that do not. The stages are 1 year olds, 2 year olds, females 3 or more years old who have yet to reproduce, reproducing females (i.e., with a yearling offspring), and females who have reproduced previously but are not reproductive in a given year.

The life cycle graph illustrating these stages is shown in Fig. 1. It corresponds to a stage-structured matrix population model

$$\mathbf{n}(t+1) = \mathbf{A}_t \mathbf{n}(t) \tag{1}$$

where $n_i(t)$ is the number of individuals in stage i at time t and $\mathbf{A}_t$ is the projection matrix from year t to year $t+1$:

$$\mathbf{A}_t = \begin{pmatrix} 0 & 0 & F_3 & F_4 & F_5 \\ G_1 & 0 & 0 & 0 & 0 \\ 0 & G_2 & P_3 & 0 & 0 \\ 0 & 0 & G_3 & P_4 & G_5 \\ 0 & 0 & 0 & G_4 & P_5 \end{pmatrix} \tag{2}$$
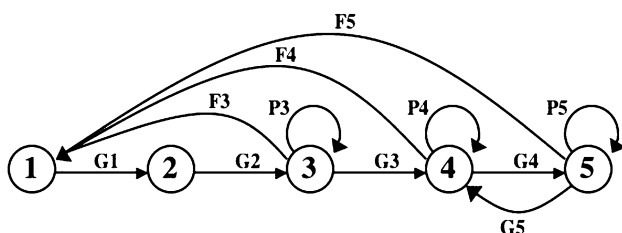

Fig. 1 Life cycle graph for female Verreaux's sifaka. Coefficients on the *arrows* form the entries of the projection matrix (Eq. 1). Stages (given in *circles*): yearlings (*1*), 2 year olds (*2*); 3 (or more)-year-old females who have not yet given birth (*3*); mothers with infants (*4*); adult females currently without infants who have given birth previously (*5*)

The coefficients G_i and P_i are defined in terms of the survival probabilities (σ_i) and transition probabilities (γ_i), as follows:

$$G_i = \gamma_i \sigma_i \tag{3}$$
$$P_i = (1 - \gamma_i)\sigma_i \tag{4}$$

The fertility F_i is the expected number of stage 1 female offspring at $t+1$ for each female in stage i at time t. Because we incorporate reproducing females as a stage in the life cycle, fertilities can be calculated from the transition probabilities of entering into stage 4 from stages 3, 4, or 5 (i.e., G_3, P_4, and G_5; these correspond to the 4,3, 4,4, and 4,5 entries in the projection matrix). Every time a female enters stage 4 she produces a female offspring with a probability of 0.46 (the observed sex ratio from 1985 to 2001). The non-zero fertilities for stages 3 and 5 represent contributions of offspring by individuals that are not reproductive in year t, but reproduce between t and $t+1$. The survival probability from birth to age 1 is incorporated into the probability of reproduction because we do not capture and mark newborn infants. Thus

$$F_i = 0.46 a_{4i} \quad i = 3, 4, 5 \tag{5}$$

Parameter estimation and goodness-of-fit

We used multi-stage mark-recapture methods to estimate the parameters. Estimates are obtained by maximizing the likelihood of a model for a given set of data, taking into account the fact that recaptures are imperfect, so that some individuals are missing from the sample but still alive. Thus the statistical models include the recapture probability (in our case, more properly called a resighting probability), denoted as $p_i(t)$ below (Lebreton et al. 1992; Fujiwara and Caswell 2002; Caswell and Fujiwara 2004). We computed the likelihood from the census histories of individual sifaka using the methods of Fujiwara and Caswell (2002; Caswell and Fujiwara 2004).

We conducted preliminary goodness-of-fit tests to assess the adequacy of the life cycle structure, following Pradel et al. (2005) and using the software U-Care (Choquet et al. 2005). These tests evaluate various assumptions of a very general model in which survival, transition, and capture probabilities are allowed to vary freely over time and to depend on both the origin and the destination stage. All of the U-Care tests were nonsignificant, indicating that our data met the assumptions of the model (3G, $\chi^2 = 44.177$, $P = 1.000$, $df = 93$; M, $\chi^2 = 2.144$, $P = 0.79$, $df = 4$; goodness-of-fit test, $\chi^2 = 46.321$, $P = 1.000$, $df = 97$).

Statistical models, model selection, and model averaging

The structure defined by the life cycle graph and the parameters σ_i, γ_i and p_i can be the basis of many statistical

models, depending on whether the parameters are constant, functions of time, or of environmental factors, or of individual organism properties. On biological grounds, we considered a set of 32 models: $\sigma_i(t)$ and $\gamma_i(t)$ may each be constant, freely time-varying, or functions of rainfall in year t or $t-1$. For each of these 16 combinations, recapture probabilities $p_i(t)$ may be constant or freely time-varying. Dependence of probabilities on rainfall was modeled using the logit transform; for example, to express $\sigma_i(t)$ as a function of rainfall $x(t)$, we write:

$$\log \frac{\sigma_i(t)}{1 - \sigma_i(t)} = \alpha_i + \beta_i x(t). \tag{6}$$

where α and β are slope and intercept parameters.

We used information-theoretic methods (Burnham and Anderson 2002) to rank the 32 statistical models examined. We calculated Akaike's information criterion (AIC) for each model, where the model with the lowest AIC provides the best and most parsimonious description of the data. We compare models using ΔAIC. Following the recommendations of Burnham and Anderson (2002), we disregard all models with ΔAIC ≥ 10. In order to include the uncertainty induced by model selection, we averaged the parameters using Akaike weights. If $\boldsymbol{\theta}_j$ is a vector containing the parameters [i.e., $\gamma_i(t)$, $\sigma_i(t)$, and $p_i(t)$] for model j, then the averaged parameters are given by $\bar{\theta} = \sum_j w_j \theta_j$, where w_j is the Akaike weight of the model j (Burnham and Anderson 2002).

Confidence intervals

We used a parametric bootstrap method to generate confidence intervals for the parameters and the demographic indices calculated from the parameters. The estimates $\hat{\theta}$ have, asymptotically, a multivariate normal distribution with mean $\boldsymbol{\theta}$ and a variance-covariance matrix $\mathbf{V}$ given by the inverse of the observed information matrix

$$\mathbf{V} = \left(\frac{\partial^2 \log L}{\partial \theta_i \partial \theta_j} \right)^{-1} \tag{7}$$

(e.g., Mood et al. 1974). To obtain confidence intervals, we generated 10,000 random parameter vectors $\boldsymbol{\theta}$ from a multivariate normal distribution with mean $\hat{\theta}$ and covariance matrix $\mathbf{V}$. For each of these parameter vectors, we generated the matrices $\mathbf{A}_t$ and from them the demographic indices of interest. The 95% confidence interval extends from the 2.5th to the 97.5th percentile of the resulting set of values. The advantage of this approach is that it propagates naturally from the θ_i to the Markov chain transition matrix (denoted as Φ_t in Fujiwara and Caswell 2002), to the $\mathbf{A}_t$ matrices, to the demographic quantities calculated from $\mathbf{A}_t$, without relying on approximations or distributional

Table 1 Delta Akaike's information criterion (ΔAIC) and Akaike weights for the top five models in our analysis

Model	ΔAIC	Akaike weight	Description
1	0.0	0.496	All parameters time invariant
2	0.7	0.421	Survival dependent on rainfall year $t-1$; growth, resighting time invariant
3	5.1	0.042	Survival, resighting time-invariant growth dependent on rainfall year t
4	5.9	0.036	Survival dependent on rainfall year $t-1$; growth dependent on rainfall year t; resighting time invariant
5	9.5	0.005	Survival dependent on rainfall year t; growth, resighting time invariant

assumptions about quantities calculated "downstream" from the θ_i.

Results

The stage-structured population model (1) can assume several forms, depending on whether parameters are time invariant, time dependent, or rainfall dependent. The top five most informative models from our model selection analysis are presented in Table 1. None of these five models included time variation in recapture, conditional transition, or survival probabilities; however, four of the five models included dependence of the lower-level vital rates γ_i and σ_i on rainfall. We first analyze the time-invariant model, which is our most informative model. Then we use the rainfall-dependent, AIC-weighted average model to study the response to constant rainfall levels. Finally, we develop a stochastic time-series model for rainfall, and use this to calculate the stochastic population growth rate (λ_s), the variance growth rate, and the sensitivity and elasticity of λ_s to lower level vital rates (σ_i and γ_i).

Time-invariant demography

The population projection matrix from the time-invariant model is:

$$\mathbf{A} = \begin{pmatrix} 0 & 0 & 0.036 & 0.159 & 0.119 \\ 0.889 & 0 & 0 & 0 & 0 \\ 0 & 0.935 & 0.798 & 0 & 0 \\ 0 & 0 & 0.079 & 0.345 & 0.258 \\ 0 & 0 & 0 & 0.633 & 0.626 \end{pmatrix} \tag{8}$$

The time-invariant model provides the best single picture of the vital rates. The survival and conditional transition probabilities are shown in Table 2. Stage-specific survival probabilities are high and show no clear pattern

with respect to stage. There is no suggestion that reproducing females have reduced survival as a cost of reproduction, but the nonbreeding mature females (stage 5) have the lowest survival probability of any stage.

Life expectancy in a stage-classified life cycle is determined by the stage-specific survival probabilities and by the amounts of time that individuals spend in each stage, which reflect the entire transition structure of the life cycle. We calculated life expectancy for each stage from the fundamental matrix (Caswell 2001, 2006). Let $\mathbf{U}$ be the matrix representing transitions only (i.e., the matrix $\mathbf{A}$ with the first row set to zero) and $\mathbf{I}$ the identity matrix. The fundamental matrix is:

$$\mathbf{N} = (\mathbf{I} - \mathbf{U})^{-1} \tag{9}$$

$$= \begin{pmatrix} 1.00 & 0 & 0 & 0 & 0 \\ 0.89 & 1.00 & 0 & 0 & 0 \\ 4.12 & 4.63 & 4.96 & 0 & 0 \\ 1.51 & 1.70 & 1.82 & 4.58 & 3.16 \\ 2.55 & 2.87 & 3.07 & 7.73 & 8.00 \end{pmatrix} \tag{10}$$

From $\mathbf{N}$ we see that a 1-year-old sifaka can expect 1.51 reproductive events in its life [the (4,1) element of $\mathbf{N}$]. The life expectancy of any stage is given by the corresponding column sum of $\mathbf{N}$ (Table 2). In this population, the life expectancy of sifaka at birth is 10.1 years.

Population growth rate is given by the dominant eigenvalue λ of $\mathbf{A}$, which in this case is $\lambda = 0.979$ with a 95% confidence interval [0.947,1.003]. The stable stage distribution $\mathbf{w}$ and the reproductive value distribution $\mathbf{v}$ are given by the right and left eigenvectors, respectively, of $\mathbf{A}$ corresponding to λ. They are given in Table 2. (The stable stage distribution can be rescaled to give the proportions of animals in each stage.) The net reproductive rate (R_0) is the expected number of female offspring produced by a female over her lifetime. It is calculated as the dominant eigenvalue of the matrix $\mathbf{R} = \mathbf{FN}$, where $\mathbf{F}$ is a matrix with fertilities F_i in the first row and zeros elsewhere (Cushing and Yicang 1994; Caswell 2001). The R_0 is less than 1 ($R_0 = 0.692$), but with a confidence interval that includes 1 (Table 2).

There are several measures of generation time (Coale 1972); here we calculate

$$\tau = \frac{\log R_o}{\log \lambda} \tag{11}$$

which is the time required for the population to grow by the amount R_0; for sifaka, $\tau = 17.5$ years (Table 2).

The sensitivities of λ to the lower level parameters σ_i and γ_i are given by, e.g.,

$$\frac{\partial \lambda}{\partial \sigma_h} = \sum_{i,j} \frac{\partial \lambda}{\partial a_{ij}} \frac{\partial a_{ij}}{\partial \sigma_h} \tag{12}$$

Table 2 Estimates and 95% confidence intervals of demographic parameters for the time-invariant model 1

Description	Estimate	95% confidence interval
Survival probability (σ)		
Stage 1 (σ_1)	0.889	0.711–0.963
Stage 2 (σ_2)	0.935	0.807–0.981
Stage 3 (σ_3)	0.878	0.849–0.902
Stage 4 (σ_4)	0.978	0.925–0.994
Stage 5 (σ_5)	0.884	0.829–0.923
Conditional transition probability (γ)		
Stage 3 (γ_3)	0.091	0.069–0.120
Stage 4 (γ_4)	0.647	0.557–0.730
Stage 5 (γ_5)	0.292	0.224–0.367
Stable stage distribution		
Stage 1	0.1512	0.124–0.180
Stage 2	0.1373	0.110–0.162
Stage 3	0.7087	0.583–0.803
Stage 4	0.3295	0.271–0.393
Stage 5	0.5895	0.472–0.711
Reproductive value		
Stage 1	1.000	1.000–1.000
Stage 2	1.102	1.012–1.365
Stage 3	1.154	1.035–1.474
Stage 4	2.156	1.586–2.980
Stage 5	1.907	1.343–2.705
Life expectancy		
Stage 1	10.063	7.537–12.408
Stage 2	10.195	8.041–12.651
Stage 3	9.838	7.866–12.464
Stage 4	12.308	8.493–17.582
Stage 5	11.161	7.487–16.434
Reproductive rate (R_o)	0.692	0.413–1.056
Generation time (τ)	17.547	14.273–22.102
Population growth rate (λ)	0.979	0.947–1.003

where the sensitivities to the matrix elements are $\partial \lambda / \partial a_{ij} = v_i w_j / \mathbf{v}^{\mathrm{T}} \mathbf{w}$. The elasticities are $\frac{\sigma_h}{\lambda} \frac{\partial \lambda}{\partial \sigma_h}$. Table 3 shows the results. Overall, λ is more sensitive and more elastic to survival probabilities rather than conditional transition probabilities. In particular, survival of stages 3, 4, and 5, are key determinants of population growth rate.

Environment-dependent demography

Four of the top five models include dependence of at least one of the vital rates on rainfall. Here we examine how population growth rate, life expectancy, and the sensitivities of λ are affected by rainfall. These calculations describe the hypothetical situation where the population

Table 3 Sensitivity and elasticity of λ with respect to lower-level demographic parameters for the time-invariant model 1

Term	Sensitivity	Elasticity
σ		
Stage 1 (σ_1)	0.056	0.051
Stage 2 (σ_2)	0.054	0.051
Stage 3 (σ_3)	0.299	0.268
Stage 4 (σ_4)	0.222	0.222
Stage 5 (σ_5)	0.395	0.356
Conditional γ		
Stage 3 (γ_3)	0.210	0.020
Stage 4 (γ_4)	−0.027	−0.018
Stage 5 (γ_5)	0.043	0.013

For symbols, see Table 2

experiences a fixed, specified level of rainfall. We explored rainfall levels from 100 to 1,400 mm per year; these values encompass the range seen in historical rainfall statistics from 1945 to 2000 (Fig. 2). The survival probabilities of stages 2, 3, and 5 are reduced at low rainfall (less than 300 mm); those of stages 1 and 4, in contrast, are slightly higher at lower rainfall levels (Fig. 3). It is not clear why these stages respond differently: intuitively one would expect infants and mothers to be more, rather than less, affected by drought (see Discussion). This question warrants more investigation. The probabilities of transition into the reproductive stage (γ_3, γ_5, and $1-\gamma_4$) increase very slightly with increasing rainfall (Fig. 3).

Both life expectancy and λ increase with increasing rainfall levels up to about 800mm and then decline at higher rainfall levels (Figs. 3, 4). When λ is calculated for the rainfall level observed in each year of the study, the result is an oscillation around the growth rate ($\lambda = 0.98$) of the time-invariant model; this oscillation tracks annual

rainfall patterns from year to year (compare rainfall from Fig. 2 years 1985–2001 to Fig. 4b). Finally, Fig. 4c shows the response of sensitivities of λ to the matrix entries corresponding to moving into stage 4 or remaining in stages 3 and 5 (these are the top four highest sensitivity values in this particular perturbation analysis). Although the sensitivities change, their relative levels are consistent for all rainfall levels above about 500 mm.

Stochastic demography

To describe the demographic consequences of a dynamic rainfall environment, we used long-term rainfall data, presented in Fig. 2, to parameterize an autoregressive moving-average (ARMA) model of (log-transformed) annual rainfall. Parameters in the ARMA model were estimated using maximum likelihood with the statistical package JMP version 5.0 (SAS Institute, Cary, N.C.). Using AIC, we found that the best fitting ARMA model was characterized by an autoregressive order of 1, and a differencing order and moving average order of 0. The resulting model is:

$$x_{t+1} = y + b(x_t - y) + \epsilon_t \qquad (13)$$

where x is log rainfall, y is the intercept, b is the autoregressive parameter, and ε is a normally distributed error term. The estimate of b is 0.208, the estimate of the intercept is 6.419, and the variance of ε is 0.1103.

To evaluate the stochastic growth rate we generated a sequence of $T = 10{,}000$ rainfall values from the time-series model (13). From this sequence we generated $\sigma_i(t)$, $\gamma_i(t)$, and $\mathbf{A}_t$ for the rainfall-dependent models in Table 1 (models 2–5). Starting with an arbitrary initial population vector, we projected the population for T years and estimated the stochastic growth rate as:

Fig. 2 Annual rainfall in Beza Mahafaly from 1946 to 2001. *Middle line* Median rainfall (614.9 mm), *upper line* upper quartile (807.5), *lower line* lower quartile (473.1)
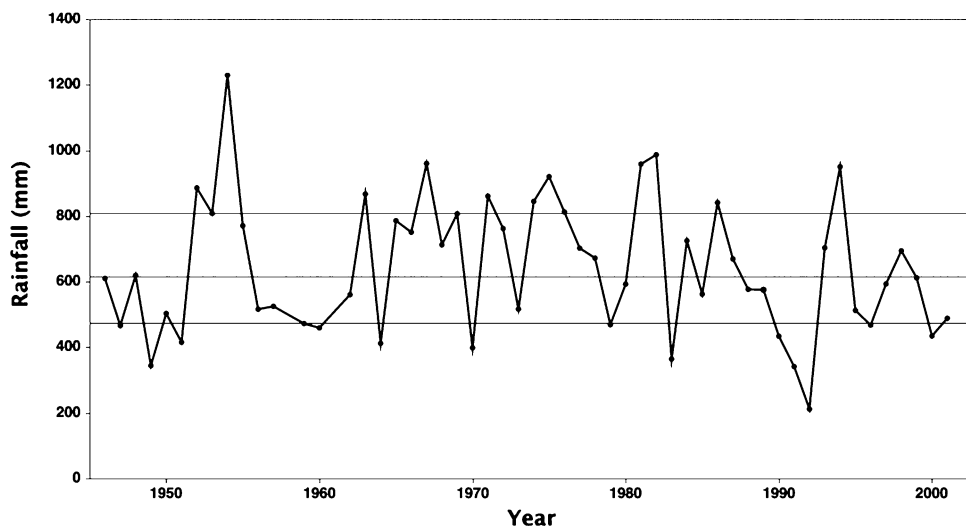
Fig. 3 Response of
demographic statistics to annual
rainfall. *Top panel* Survival
probabilities (σ); *middle panel*
transition probabilities (γ);
bottom panel life expectancy,
as functions of rainfall
calculated from the average
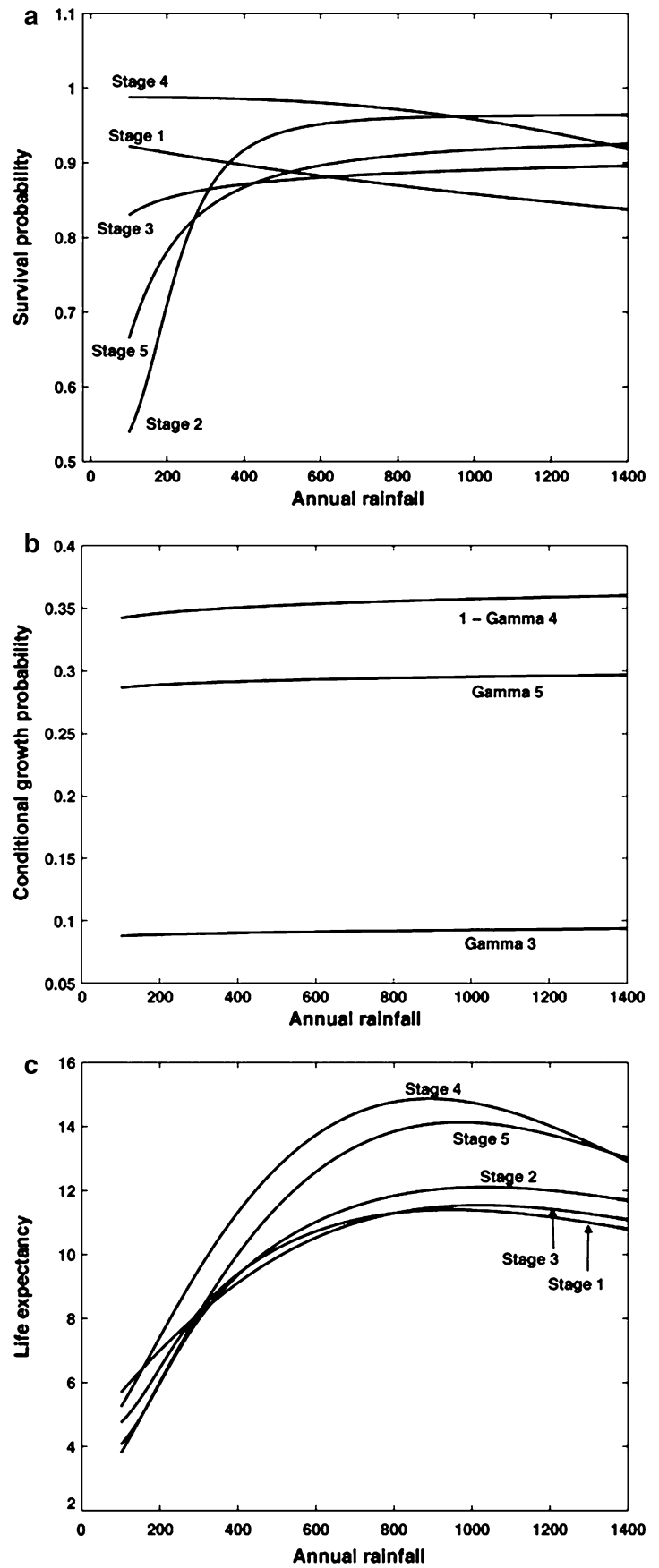model

Fig. 4 Response of demographic statistics to annual rainfall and temporal variation. *Top panel* Population growth rate (λ) from the average model as a function of rainfall; *middle panel* λ from the average model and models 1 and 2 as a function of time; *bottom panel* four highest sensitivities of λ to matrix entries, calculated from the average model

Table 4 Stochastic growth rate (λ_s), the variance growth rate (σ^2), and 95% parametric bootstrap confidence intervals for λ_s for rainfall-dependent models (models 2–5)

Model	λ_s	σ^2	95% confidence interval for λ_s
2	0.9849	6.25×10^{-5}	0.9357–1.0037
3	0.9812	1.39×10^{-4}	0.9450–1.0078
4	0.9866	3.46×10^{-5}	0.9347–0.9985
5	0.9789	1.53×10^{-4}	0.9468–1.0034

$$\widehat{\log \lambda_s} = \frac{1}{T} \sum_{i=0}^{T-1} \log r(t) \qquad (14)$$

where $r(t) = \|\mathbf{n}(t+1)\|/\|\mathbf{n}(t)\|$. We used the parametric bootstrap procedure to calculate 95% confidence intervals on λ_s, with a bootstrap sample size of 1,000. We calculated the sensitivities of log λ_s and the elasticities of λ_s to the lower level parameters that define each matrix entry using Eqs. 14 and 15 of Caswell (2005). The log of population size is asymptotically normally distributed with a variance that increases linearly at a rate denoted σ^2 (Tuljapurkar and Orzack 1980). We estimated σ^2 using the Heyde-Cohen estimator (Heyde and Cohen 1985; cf. Eq. 14.80 of Caswell 2001).

The stochastic growth rates λ_s for the four models lie between 0.97 and 0.99 (Table 4) with broadly overlapping

confidence intervals. The lowest is produced by model 5, in which survival depends on the current year's rainfall ($\lambda_s = 0.9789$). The highest is produced by model 4, in which survival depends on the previous year's rainfall and growth depends on the current year's rainfall ($\lambda_s = 0.9866$). The variance growth rate is extremely small for all models ($\sigma^2 < 1.0 \times 10^{-4}$); these small values are consistent with other populations of long-lived vertebrates (H. Caswell, unpublished data). Figures 5 and 6 show the sensitivity of λ_s and elasticity of λ_s to perturbations to lower level parameters (i.e., σ and γ) for each model. Because model 1 is time invariant, it is unaffected by the stochastic environment, but the pattern of sensitivities and elasticities is very similar between the time-invariant and the stochastic models.

The λ_s calculations are based on the estimated variance in the noise term ε in the autoregressive model (13). By changing this variance, we can explore the dependence of the stochastic growth rate on environmental variability (Fig. 7). There are several highly nonlinear steps between the variance in ε and the variance in the entries of $\mathbf{A}_t$, so this manipulation does not constitute a change in variance keeping the mean demography constant. Thus the response of log λ_s to the variance in ε can be either negative or positive (cf. Efford 2001; Ripley and Caswell 2006).

The time-invariant model 1 is, of course, independent of the variance. In models 2, 4, and 5, log λ_s declines with

Fig. 5 Sensitivity of the stochastic growth rate (λ_s) to changes in lower level vital rates (σ and γ) for each model in Table 1, with environmental stochasticity generated by the autoregressive moving-average (ARMA) model for annual rainfall. For symbols, see Table 3
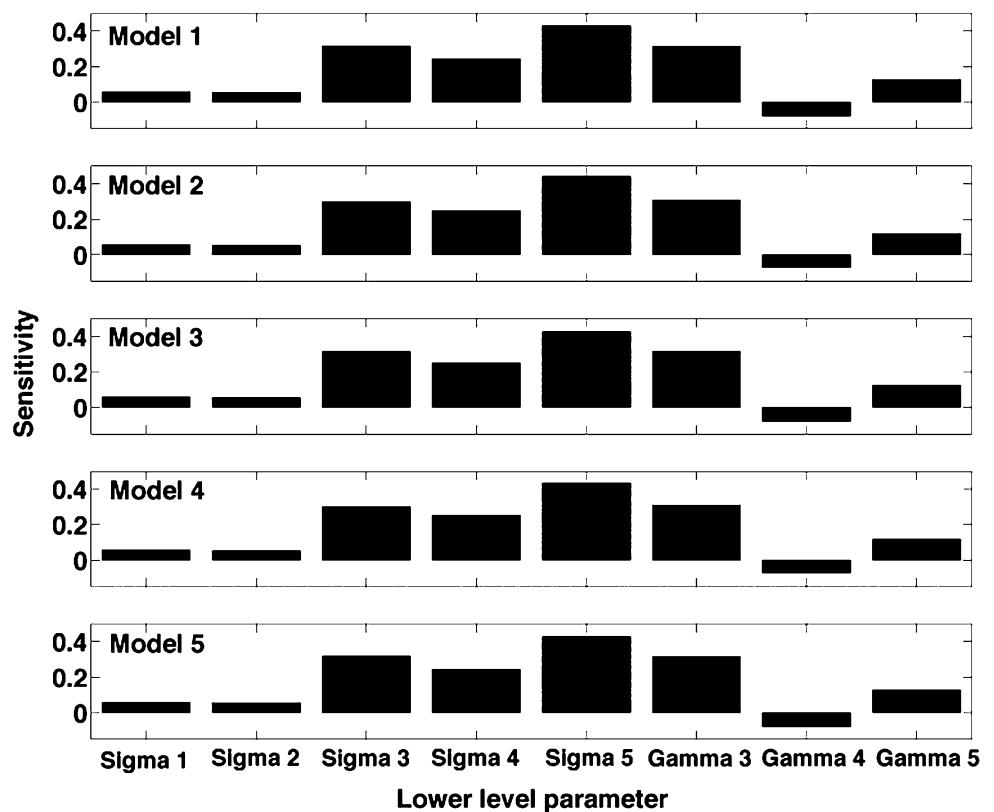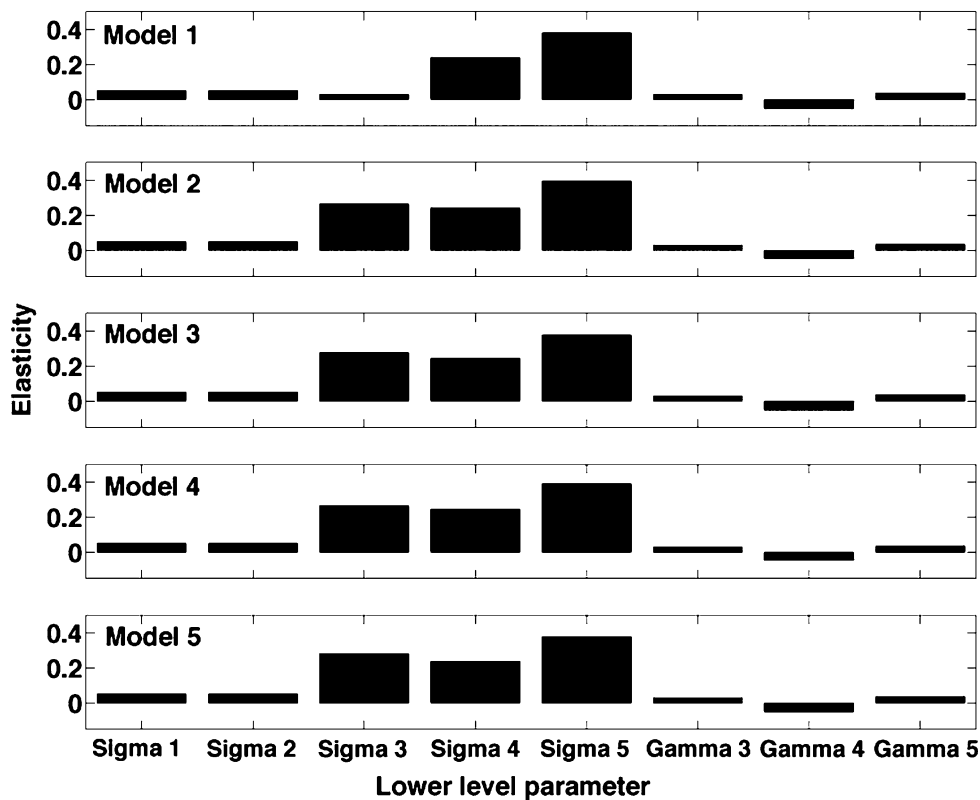
Fig. 6 Elasticity of λ_s to changes in lower level vital rates (σ and γ) for each model in Table 1, with environmental stochasticity generated by the ARMA model for annual rainfall. For symbols, see Table 3

increasing variance. Model 3 exhibits a slight increase in log λ_s with increasing variance. Since model 2 carries the largest Akaike weight of any of the environment-dependent models (Table 1), and model 1 is independent of the variance, the overall picture from models 1 and 2 (both which have large Akaike weights relative to the other models) indicates a decrease in long-term stochastic growth as a result of increased variance in rainfall.

Discussion

All of our analyses concur in finding a population growth rate, deterministic or stochastic, of around 0.98 per year, implying a population decline of about 2% per year. This raises interesting questions of interpretation. If the population growth rate is truly negative, the population is in serious jeopardy. On the other hand, if the population were at a stable equilibrium, λ would equal 1.0 and the population would be relatively safe. In our case, the 95% confidence intervals for the time-invariant model, and for three of the four stochastic models, include 1.0. Confidence intervals for the average model are not shown, but they would be wider than those for the time-invariant model, since they include both model uncertainty and parameter uncertainty (Burnham and Anderson 2002), and so would also include 1.0. Thus we cannot conclude that population

growth is negative, but we certainly have no strong evidence that it is positive.

It is not clear how a properly risk-averse conservation biologist should view these results. Growth rates significantly below replacement are a clear sign that a population is at risk. But in this case, is it appropriate to conclude that λ is not clearly less than 1, and hence that the population cannot be said to be declining? Or is it better to say that λ is not clearly greater than 1, and hence that the population cannot be said to be increasing? Based on our model selection results, it seems safe to say that λ hovers slightly below 1 but that the population is not in immediate danger of extinction. It is important to note that we made no attempt to estimate immigration and emigration in this population, and more detailed analyses of this problem are forthcoming.

Our perturbation analyses (of the time-invariant, environment-dependent, and stochastic models) conclude that transitions among stages 3, 4, and 5 are key determinants of population growth rate. This pattern mirrors those of many other long-lived species in that perturbations to adult survival have a larger impact on population growth rate than juvenile survival or adult fertility (e.g., Crouse et al. 1987; Brault and Caswell 1993). Examination of lower level parameters reveals that λ is slightly more sensitive to survival (σ_i) of stages 3, 4, and 5, than to transitions among these stages (e.g., γ_3, γ_4). The

Fig. 7 The stochastic population growth rate (log λ_s) as a function of variance in annual rainfall for each model in Table 1

relatively high sensitivity of λ and λ_s to γ_3, the rate of first reproduction, suggests that age at first reproduction is, all else being equal, under strong directional selection (Lande 1982). All else is not, of course, equal, and it would be interesting to explore trade-offs between early reproduction and other life history traits.

Population growth rate is determined by the vital rates—the rates of birth, growth, maturation, fertility, and mortality. As is evident from Figs. 3 and 4, the response of the demographic parameters to rainfall is most sensitive below 300 mm. These include adult survival, life expectancy, population growth rate, directional selection on stages P_3, P_5, G_3, G_5, and reproductive value (the latter of which is not shown). Rainfall probably influences the vital rates through food availability. The availability of young leaves and fruit is positively correlated with annual rainfall at our field site (Sauther 1998). Periods of low rainfall are associated with low food availability, which in turn impacts female feeding competition, female body mass, and the probability of giving birth (Richard et al. 2000); low food availability also plays a role in infant and adult survival, along with other factors such as predation (Richard et al. 2002; Brockman et al. 2008). Life expectancy and, to a lesser extent, λ show concave relationships with rainfall. High annual rainfall is associated with tropical cyclones, and prolonged rainfall during cyclone years may induce hypothermia (Richard et al. 2002); this likely explains the negative response to high annual rainfall.

Studies of intra- and interannual rainfall indicate that Madagascar, particularly southwest Madagascar, is characterized by very low predictability of rainfall from month to month (Dewar and Wallis 1999; Dewar and Richard 2007). Our analyses show how variation in rainfall influences lemur population growth. Given that rainfall patterns influence primary productivity of the sifaka forest and hence food resources, periods of low rainfall can disrupt population growth via the food supply. Not all lemur species will respond in the same way to variation in rainfall. For example, the folivorous sifaka contrasts with the frugivorous ringtail lemur (*Lemur catta*), which is also found at Beza Mahafaly Special Reserve. Ringtail infants grow more rapidly and are weaned at a higher body mass than sifaka infants, suggesting maternal investment is higher in ringtails than in sifaka. Additionally, observations in the wild and in captivity indicate that female ringtails reproduce earlier and more often than female sifaka and overall lifespan is shorter in ringtails than for sifaka (Godfrey et al. 2004). Summarizing information from ecological studies of both species, Godfrey et al. (2004) argue that they follow different patterns of recovery after a population crash such as a drought. Ringtail lemurs recover faster than sifaka; ringtails also incur comparably more mortality across all age classes during droughts than sifaka. This likely is due to the fact that fruit supplies are more severely depleted than leaves during drought years (Godfrey et al. 2004). Thus despite living in the same habitat that is characterized

by unpredictable periods of low rainfall (Dewar and Wallis 1999; Dewar and Richard 2007), these two species have different demographic responses to drought.

Rainfall over the last 50 years has fluctuated widely (Fig. 2) and on at least three occasions has fallen below 400mm, producing drought-like conditions. If past droughts have had the same effect as the documented effect of the 1992 drought (Fig. 2; and Gould et al. 1999; Richard et al. 2002), these lemur species may experience non-equilibrium conditions. Interestingly, the patterns of recovery and population growth that characterize ringtails and sifaka are similar to the two nonequilibrium demographic patterns discussed in Caswell (1982). Ringtails, it appears, spend most of their demographic history increasing from recurrent and severe population crashes. Sifaka, on the other hand, spend most of their demographic history in a state of slow decline (see Fig. 1 in Caswell 1982). Caswell's theoretical analysis of nonequilibrium life history evolution maps on to the empirical patterns documented for ringtails and sifaka, in that, "the traits favored in declining populations include long lifespan, slow development, delayed reproduction, iteroparity, low degree of senescence, and perhaps a relatively high degree of investment of whatever offspring are produced. The traits favored in increasing nonequilibrium populations are largely the opposite..." (Caswell 1982, p. 336). Richard et al. (2002) have shown that, when controlling for body size, sifaka live longer and begin reproducing later than all other primate species for which there are comparable data (also see Table 2).

Indeed Madagascar's mammals might all be characterized as nonequilibrium species by virtue of the "hyper-variable" rainfall patterns (Dewar and Richard 2007). When compared to related species from other regions, Malagasy mammal species are characterized by either extreme "fastness" or extreme "slowness" in their life history schedules (Dewar and Richard 2007). Since rainfall is a potentially major driver of these divergent life history patterns, it is important to understand how demographic patterns are shaped by variation in rainfall (see King et al. 2005 for another example of how rainfall impinges on lemur livelihoods). The demographic analyses in this study provide an empirical framework for the analysis of life history patterns in (potentially) nonequilibrium populations.

Model averaging provides a way to include information from the best models in our analysis, of which four show some rainfall dependence. By plotting how demographic factors as well as the strength of selection changes as a function of annual rainfall, we can gain insight into the climate processes that shape population dynamics. Further, our time-series analysis provides a means to calculate the stochastic population growth rate (λ_s), the sensitivity and elasticity of λ_s to changes in survival and growth, and how

λ_s changes with changes in the variance in rainfall. Given their noticeable effects on population structure, most previous studies of primate populations and climate have focused on how extreme climate events such as droughts impinge on primate populations over a short time interval (e.g., Gould et al. 1999; Richard et al. 2002; Jolly et al. 2002). In contrast, our analysis documents how a primate population is influenced by the entire range of rainfall values as well as stochastic fluctuations as revealed in 50 years of rainfall data.

Stochastic models like ours can, when linked to forecasts from global climate models, project population responses to climate change (e.g., Hunter et al. 2007; also see Morris et al. 2008). Such analyses will be particularly important in light of the predictions by many climate models of a decrease in mean annual rainfall in southern Madagascar (Hudson and Jones 2002; Hoerling et al. 2006). Climate change is predicted to produce increases in the variance of such variables as temperature and precipitation, as well as trends in the mean (e.g. Raisanen 2002; Watterson 2005). In the case of sifaka, if climate change reduces the mean or increases the variance in rainfall, the result will be a distinctly negative effect on population growth. Stochastic models including links to explicit time-series models of the environment have great potential for exploring such effects of variability on population growth, and can allow researchers to anticipate rather than respond to population disturbances brought about by climate change.

References

Alberts SC, Altmann J (2003) Matrix models for primate life history analysis. In: Kappeler PM, Pereira ME (eds) Primate life histories and socioecology. University of Chicago Press, Chicago, pp 66–102

Anderson DR (2008) Model based inference in the life sciences: a primer on evidence. Springer, New York

Brault S, Caswell H (1993) Pod-specific demography of killer whales (*Orcinus orca*). Ecology 74:1444–1454

Brockman DK, Dollar LJ, Godfrey LR (2008) Evidence of wildcat (*Felis silvestris*) predation on *Propithecus verreauxi* at Beza Mahafaly, Madagascar. Int J Primatol 29:135–152

Burnham KP, Anderson DR (2002) Model selection and multimodel inference. A practical information theoretic approach. Springer, Berlin

Caswell H (1982) Life history theory and the equilibrium status of populations. Am Nat 120:317–339

Caswell H (2001) Matrix population models. Sinauer, Sunderland

Caswell H (2005) Sensitivity analysis of the stochastic growth rate: three extensions. Aust NZ J Stat 47:75–85

Caswell H (2006) Applications of Markov chains in demography. In: Langville AN, Stewart WJ (eds) MAM2006: Markov Anniversary Meeting. Boson Books, Raleigh, pp 319–334

Caswell H, Fujiwara M (2004) Beyond survival estimation: mark-recapture, matrix population models, and population dynamics. Anim Biodiv Cons 27:471–488

Caswell H, Takada T, Hunter CM (2004) Sensitivity analysis of equilibrium in density-dependent matrix population models. Ecol Lett 7:380–387

Choquet R, Reboulet A-M, Lebreton J-D, Gimenez O, Pradel R (2005) U-Care 2.2 user's manual. CEFE, Montpelier

Coale AJ (1972) The growth and structure of human populations: a mathematical approach. Princeton University Press, Princeton

Cowlishaw G, Dunbar RIM (2000) Primate conservation biology. University of Chicago Press, Chicago

Crouse DT, Crowder LB, Caswell H (1987) A stage-based population model for loggerhead sea turtles and implications for conservation. Ecology 68:1412–1423

Cushing JM, Yicang Z (1994) The net reproductive value and stability in matrix population models. Nat Res Mod 8:297–333

Dewar RE, Wallis JR (1999) Geographical patterning of interannual rainfall variability in the tropics and near tropics: an L-moments approach. J Clim 12:3457–3466

Dewar RE, Richard AF (2007) Evolution in the hypervariable environment of Madagascar. Proc Natl Acad Sci USA 104:13723–13727

Dobson AP, Lyles AM (1989) The population dynamics and conservation of primate populations. Cons Biol 3:362–381

Efford M (2001) Environmental stochasticity cannot save declining populations. Trends Ecol Evol 16:177

Fujiwara M, Caswell H (2002) Estimating population projection matrices from multi-stage mark-recapture data. Ecology 83:3257–3265

Gage TB (1998) The comparative demography of primates: with some comments on the evolution of life histories. Annu Rev Anthropol 27:197–221

Ganzhorn JU (1995) Cyclones over Madagascar: fate or fortune? Ambio 24:124–125

Godfrey LR, Samonds KE, Jungers WL, Sutherland MR, Irwin MT (2004) Ontogenetic correlates of diet in Malagasy lemurs. Am J Phys Anthropol 123:250–276

Gould L, Sussman RW, Sauther ML (1999) Natural disasters and primate populations: the effects of a 2-year drought on a naturally occurring population of ring-tailed lemurs (*Lemur catta*) in southwestern Madagascar. Int J Primatol 20:69–84

Gould L, Sussman RW, Sauther ML (2003) Demographic and life-history patterns in a population of ring-tailed lemurs (*Lemur catta*) at Beza Mahafaly Reserve, Madagascar: a 15-year perspective. Am J Phys Anthropol 120:182–194.

Heyde CC, Cohen JE (1985) Confidence intervals for demographic projections based on products of random matrices. Theor Pop Biol 27:120–153

Hoerling MP, Hurrell JW, Eischeid J (2006) Detection and attribution of 20th century northern and southern African monsoon change. J Clim 19:3989–4008

Hudson DA, Jones RG (2002) Regional climate model simulations of present-day and future climates of southern Africa. Hadley Centre Tech Note 39:1–42

Hunter CM, Caswell H, Runge MC, Regehr EV, Amstrup SC, Stirling I (2007) Polar bears in the southern Beaufort Sea. II. Demography and population growth in relation to sea ice conditions. U.S.G.S. administrative report, 1–42

Jolly A, Dobson A, Rasamimmanana HM, Walker J, O'Connor S, Solberg M, Perel V (2002) Demography of *Lemur catta* at Berenty Reserve, Madagascar: effect of troop size, habitat, and rainfall. Int J Primatol 23:327–353

Kappeler PM (1996) Causes and consequences of life history variation among strepsirhing primates. Am Nat 148:868–891

King SJ, Arrigo-Nelson SJ, Pochron ST, Semprebon GM, Godfrey LR, Wright PC, Jernvall J (2005) Dental senescence in a long-lived primate links infant survival to rainfall. Proc Nat Acad Sci USA 102:16579–16583

Lande R (1982) A quantitative genetic theory of life history evolution. Ecology 63:607–615

Lebreton J-D, Burnham KP, Clobert J, Anderson DR, (1992) Modeling survival and testing biological hypotheses using marked animals: a unified approach with case studies. Ecol Monogr 62:67–118

Mittermeier RA, Konstant WR, Hawkins F, Louis EE, Langrand O, Ratsimbazafy J, Rasoloarison R, Ganzhorn JU, Rajaobelina S, Tattersall I, Meyer DM (2006) Lemurs of Madagascar. (Tropical field guide series) Conservation International, Washington DC

Mood AM, Graybill FA, Boes DC (1974) Introduction to the theory of statistics. McGraw Hill, New York

Morris WF, Pfister CA, Tuljapurkar S, Haridas CV, Boggs CL, Boyce MS, Bruna EM, Church DR, Coulson T, Doak DF, Forsyth S, Gaillard J-M, Horvitz CC, Kalisz S, Kendall BE, Knight TM, Lee CT, Menges ES (2008) Longevity can buffer plant and animal populations against changing climatic variability. Ecology 89:19–25

Pradel R, Gimenez O, Lebreton J-D (2005) Principles and interest of GOF tests for multistate capture-recapture models. Anim Biodiv Cons 28:189–204

Pochron ST, Tucker WT, Wright PC (2004) Demography, life history, and social structure in *Propithecus diadema edwardsi* from 1986-2000 in Ranomafana National Park, Madagascar. Am J Phys Anthropol 125:61–72

Raisanen J (2002) CO_2-induced changes in interannual temperature and precipitation variability in 19 CMIP2 experiments. J Clim 15:2395–2411

Richard AF, Dewar RE (1990) Lemur ecology. Annu Rev Ecol Syst 22:145–175

Richard AF, Dewar RE, Schwartz M, Ratsirarson J (2000) Mass change, environmental variability and female fertility in wild *Propithecus verreauxi*. J Hum Evol 39:381–391

Richard AF, Dewar RE, Schwartz M, Ratsirarson J (2002) Life in the slow lane? Demography and life histories of male and female sifaka (*Propithecus verreauxi verreauxi*). J Zool 256:421–436

Ripley BJ, Caswell H (2006) Recruitment variability and stochastic population growth of the soft-shell clam *Mya arenaria*. Ecol Mod 193:517–530

Sauther ML (1998) Interplay of phenology and reproduction in ring-tailed lemurs: implications for ring-tailed lemur conservation. Folia Primatol 69:309–320

Strier KB, Boubli JP, Possamai CB, Mendes SL (2006) Population demography of Northern Muriquis (*Brachyteles hypoxanthus*) at the Estacao Biologica de Caratinga/Reserva Particular do

Patrimonio Natural-Feliciano Miguel Abdala, Minas Gerais, Brazil. Am J Phys Anthropol 130:227–237

Tuljapurkar S, Orzack SH (1980) Population dynamics in variable environments. I. Long-run growth rates and extinction. Theor Pop Biol 18:314–342

Watterson IG (2005) Simulated changes due to globals warming in the variability of precipitation, and their interpretation using a gamma-distributed stochastic model. Adv Water Res 28:1368–1381

Wich SA, Steenbeck R, Sterck EH, Korstjens AH, Willem EP, Van Schaik CP (2007) Demography and life history of Thomas langurs (*Presbytis thomasi*). Am J Primatol 69:641–651

Wright PC (1999) Lemur traits and Madagascar ecology: coping with an island environment. Yrbk Phys Anthropol 42:31–72